

Synthesis, Characterization And Crystallographic Features Of Zirconium Molybdo-Pyrophosphate As A Composite Material

¹M. M. Abou-Mesalam, ²M.M El-Shorbagy, ³R.A.Abou-lilah, ⁴NagdaHossny & ⁵N.A.Badway

^{1,2,3}Atomic Energy Authority, Hot Labs. Centre, P. Code 13759, Cairo, Egypt

^{4,5}Al-Azhar University, Faculty of Science, Chemistry Department, Cairo, Egypt

Email- mabumesalam@yahoo.com

Abstract

A three inorganic ion exchange materials zirconium phosphate, zirconium molybdate and zirconium molybdo-pyrophosphate have been synthesized under identical conditions. Structures of these materials were established by chemical analysis, X-ray diffraction, thermogravimetric and differential thermal analyses, fourier transform infrared spectroscopy and X-ray fluorescence analysis. From the data obtained the synthesized materials can be written as $(Zr_{1.15}PO_{4.8}.3H_2O)$ for zirconium phosphate with an amorphous structure and $(Zr_{1.18}Mo_{0.7}.2H_2O)$ and $(Zr_{1.7}MoPO_{7.2}.3H_2O)$ for zirconium molybdate and zirconium molybdo-pyrophosphate, respectively, with the semicrystalline structures. The data obtained from X-ray peak broadening analysis was used to evaluate the crystallite size and lattice strain by Scherer's formula and Williamson-Hall (W.H) analyses. The chemical stability of these materials has been investigated in water and acidic media. The ion exchange capacity of zirconium molybdo-pyrophosphate for Pb^{2+} and Cd^{2+} ions have been studied at different heating temperatures.

Keywords: - Synthesis, Characterization, Crystallographic Features, Zirconium Molybdo-Pyrophosphate, Composite Material.

1- INTRODUCTION

A good deal of interest has grown in the last decades in synthetic inorganic ion-exchangers because of their greater resistance to high radiation and high temperature, which is of great importance in the nuclear technology [1]. Inorganic ion-exchangers have been widely used for the removal of heavy toxic metals from wastewater [2]. The water pollution also arises due to the increasing use of copper, iron, zinc, lead and cadmium in many industries [3]. The heavy metals when present in water are injurious to the health. Thus, by synthesizing new inorganic cation-exchangers, having affinity and selectivity for a particular metal ion, one can separate the undesired metal from effluents. Zirconium molybdo-pyrophosphate (ZMPP) ion exchanger

dried at 50 °C was used in the removal of ^{134}Cs , ^{60}Co and $^{152,154}Eu$ radioisotopes from radioactive liquid waste solutions with the selectivity $Cs(I) > Eu(III) > Co(II)$ [4]. In this work three inorganic ion exchangers based on phosphate and molybdate anions such as zirconium phosphate, zirconium molybdate and zirconium molybdo-pyrophosphate were studied. These components were found to show relatively increased ion-exchange capacity and selectivity. The present paper describes the synthesis of inorganic ion exchange materials in different volume ratios. Chemical stability, crystallite size and lattice strain was investigated. The empirical formulas, structures and the ion-exchange capacities of the product materials were conducted.

2- EXPERIMENTAL

All reagents were of analytical grade and used without further purification.

2.1- SYNTHESIS OF INORGANIC ION EXCHANGERS

Zirconium phosphate (ZP) and zirconium molybdate (ZM) were prepared by drop wise addition of equimolar solutions (0.1M) of sodium phosphate or sodium molybdate (Na_2MoO_4) to zirconium oxychloride (ZrOCl_2) with volumetric ratio Zr/P or Zr/Mo equal to unity at constant stirring and room temperature. On the other hand, zirconium molybdo-pyrophosphate was prepared by dropwise addition of equimolar solutions (0.1M) of zirconium oxychloride (ZrOCl_2) and sodium molybdate (Na_2MoO_4) to tetra sodium pyrophosphate ($\text{Na}_4\text{P}_2\text{O}_7$) with volumetric ratio Zr:MO:P equal to 2:1:1 at constant stirring and room temperature. After complete addition precipitation was occurred and then the reaction mixtures were overnight standing. The precipitates were filtered and washed several times with deionized water. The precipitate was dried at 50°C in an electric oven, grained and sieved for different mesh sizes and stored at room temperature.

2.2- IDENTIFICATION OF THE COMPOSITION OF THE PREPARED MATERIALS

Powdered X-ray Diffraction (XRD) was used for identification of the crystal phase. The XRD measurements were performed on a Shimadzu XD-D1, X-ray diffractometer with $\text{Cu-K}\alpha$ radiation with $\lambda = 1.5406 \text{ \AA}$ at scanning rate $2^\circ/\text{min}$. A differential thermal and thermogravimetric analysis of Zirconium phosphate (ZP), zirconium molybdate (ZM) and zirconium molybdo pyrophosphate (ZMPP) were carried out using a Shimadzu DTA and TGA thermal analyzer. The elemental analysis of the prepared materials was investigated using a Philips sequential X-ray spectrometer-2400. Infrared spectra of the samples were measured in the frequency range $400\text{-}4000 \text{ cm}^{-1}$ using a

pellets disk method and spectra were recorded on a Fourier Transform-series [5].

2.3- CHEMICAL STABILITY

The stability of zirconium phosphate (ZP), zirconium molybdate (ZM) and zirconium molybdo pyrophosphate (ZMPP) in various media such as H_2O , HCl and HNO_3 were studied by mixing 0.05 gm of the solid with 5 ml of the desired solution using a batch factor equal 100 ml.g^{-1} in a shaker thermostat at $25 \pm 1^\circ\text{C}$ for 72 hours. The concentration of the acid was varied between 0.1 to 6 M. After 3 days the solution was separated by centrifugation and the solutions analyzed by atomic absorption spectrometer (AAS) for determination of the metal ion concentration in solution.

2.4- CAPACITY MEASUREMENTS

Repeated batch equilibration of 30 ppm metal Chloride solution (Pb^{+2} and Cd^{+2}) with solid material in V/m ratio 100 ml/g was carried out for the capacity evaluation. The mixture was shaken in a shaker thermostat at $25 \pm 1^\circ\text{C}$. After overnight standing the solid was separated and the concentration of the metal ion was measured by atomic absorption spectrometer (AAS). The capacity value was calculated by Equation (1):

$$\text{Capacity} = \text{Uptake} \times C_0 \times V/m \quad (1)$$

Where C_0 is the initial concentration of solution (mg/l), V is the solution volume (ml) and m is the weight of the exchanger (g) [6,7].

3- RESULTS AND DISCUSSION

The scope of this work is the attempt to synthesize composites with high chemical stability and high selectivity for some pollutants and heavy metals [8]. The exchangers zirconium phosphate (ZP), zirconium molybdate (ZM) and zirconium molybdo pyrophosphate (ZMPP) were synthesized with complete characterization for elucidation the structure and the chemical formula of the composites.

The chemical stability of ZP, ZM and ZMPP were studied in water, nitric acid and hydrochloric acid and the data showed high stability to chemical attack. The

composites are stable in HNO₃ and HCl solutions up to 3 M acid solutions.

X-ray diffraction patterns of ZP, ZM and ZMPP are represented in Figs.(1,2,3). Figures 2 and 3 show that the composites ZM and ZMPP have semi crystalline nature while ZP has the amorphous structure. The XRD pattern of ZMPP heated at different heating temperatures

50°C, 200°C, 400°C, 600°C, 850°C and after saturated by 30ppm of Pb²⁺ and Cd²⁺ ions show that ZMPP have amorphous structure up to 600°C and crystallinity increased at 600°C, 850°C. The Bragg angle 2θ and the full width at half maximum β(FWHM) were determined to evaluate the crystalline size and lattice strain for the material. From Debe-Scherrer,s formula;

$$D = (K \cdot \lambda) / \beta \cdot \cos \theta \quad (2)$$

Where D is the effective average crystalline size, K is the shape factor (0.9), λ is the wavelength of Cu-K_α radiation in Å, θ is the Bragg diffraction angle and the β is the measured full width at half maximum(FWHM). The lattice strain induced in powders due to crystal imperfection and distortion was calculated using Hall equation with the formula[9,10].

$$\beta \cos \theta / \lambda = 1/D + (\epsilon \cdot \sin \theta) / \lambda \quad (3)$$

where ε is the effective strain. By substitution in equation 2 from equation 1 about the value of (ε), equation 3 becomes; $(\beta \cdot \cos \theta) / \lambda = \{ (\beta \cdot \cos \theta) / (K \cdot \lambda) \} + \{ (\epsilon \cdot \sin \theta) / \lambda \}$

By multiplying both sides of equation 3 in a constant value λ / (β · cos θ) and

Table (1) Crystalline size and Lattice strain for ZMPP before and after saturation by Pb²⁺ and Cd²⁺ ions.

Temperature °C	Crystalline size			Strain		
	Before satu.	After satu.		Before satu.	After satu.	
		by Pb	by Cd		by Pb	by Cd
50 °C	Amor.	Amor.	Amor.	Amor.	Amor.	Amor.
200 °C	Amor.	Amor.	Amor.	Amor.	Amor.	Amor.
400 °C	Amor.	Amor.	Amor.	Amor.	Amor.	Amor.
600 °C	0.396	0.46	0.81	2	1.6	0.5

rearrangement we get on;

$$\epsilon = \beta / 4 \tan \theta \quad (5)$$

From equation 2 and 5 it was confirmed that the peak width from crystalline size varies as 1/ Cos θ strain varies as tan θ. The sum of the equations 2 and 5.

$$\beta = \{ K \cdot \lambda / D \cos \theta \} + 4 \epsilon \cdot \tan \theta \quad (6)$$

By rearranging the above equation, we get;

$$\beta \cos \theta = \{ K \cdot \lambda / D \} + 4 \epsilon \sin \theta \quad (7)$$

The above equations are Williamson-Hall,s (W-H) equations.

By plots relation between (4 sin θ) along x-axis and (β cos θ) along y-axis and from the linear fit of the data, the crystalline size was estimated from the y- intercept, and the lattice strain (ε), from the slope of the fit was calculated and the results represented in Table(1). The data in Table(1) indicated that opposite order with and the lattice strain of ZMPP heated at different crystalline size heating temperatures before and after saturation by 30ppm of Pb²⁺ and Cd²⁺ ions. The data in Table(1) show that the lattice strain (ε) before saturation > (ε) after saturation by Pb²⁺ ion > (ε) after saturation by Cd²⁺ ion. This order shows that opposite order with crystalline size[11].

IR spectrums of the composites were represented in Figs. (4,5 and 6). From Figs.(4 and 5) we found that broad and sharp peak in the range 3600-3200 and ~1620 cm⁻¹, which assigned to the stretching and bending modes of water molecules [12]. In Fig.(4) a band in the region 1050 cm⁻¹ may be due to the presence of P-O stretching

850 °C	0.346	0.4	0.77	3	2.38	0.75
--------	-------	-----	------	---	------	------

N.B.; Amor. : Amorphous and Satu. : Saturation

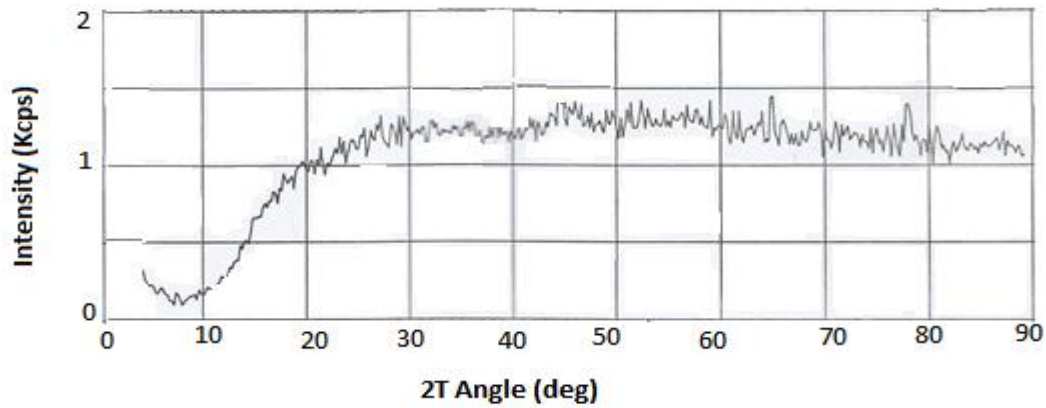


Fig.(1): XRD pattern of zirconium phosphate (ZP) composite

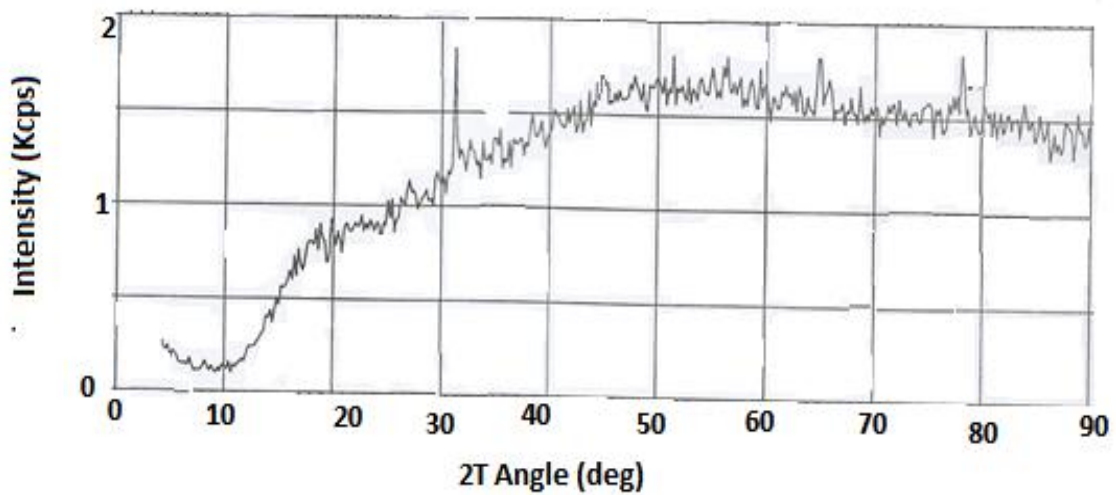


Fig.(2): XRD pattern of zirconium molybdate (ZM) composite

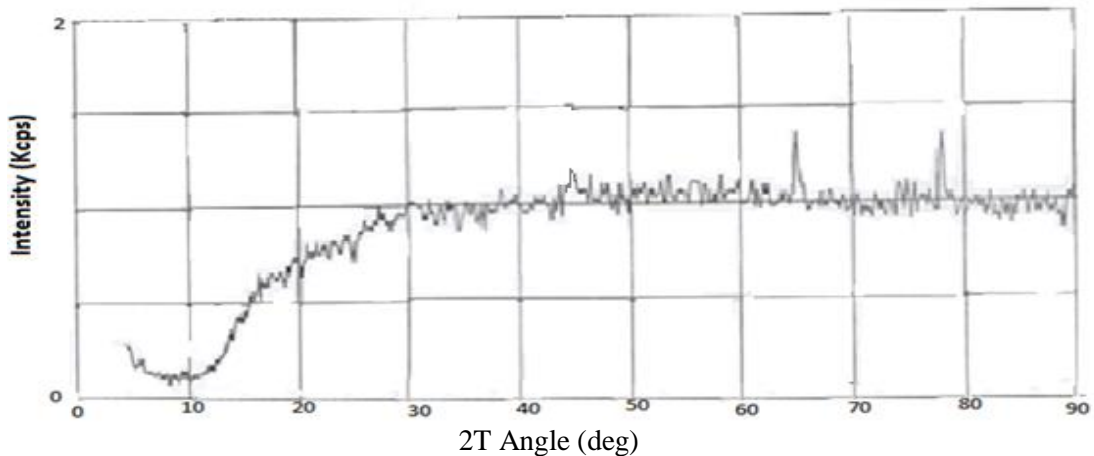


Fig.(3): XRD pattern of zirconium molybdo pyrophosphate phosphate (ZMPP) composite

[13]. In Fig.6 we found that broad and sharp peak in the range 3600-2600 and ~ 1600 cm^{-1} , which assigned to free and interstitial water molecules. The peaks at 880 and 740 cm^{-1} due to Zr-O bond. The peak at 500 due to Mo-O bond and characterized to molybdate group [14].

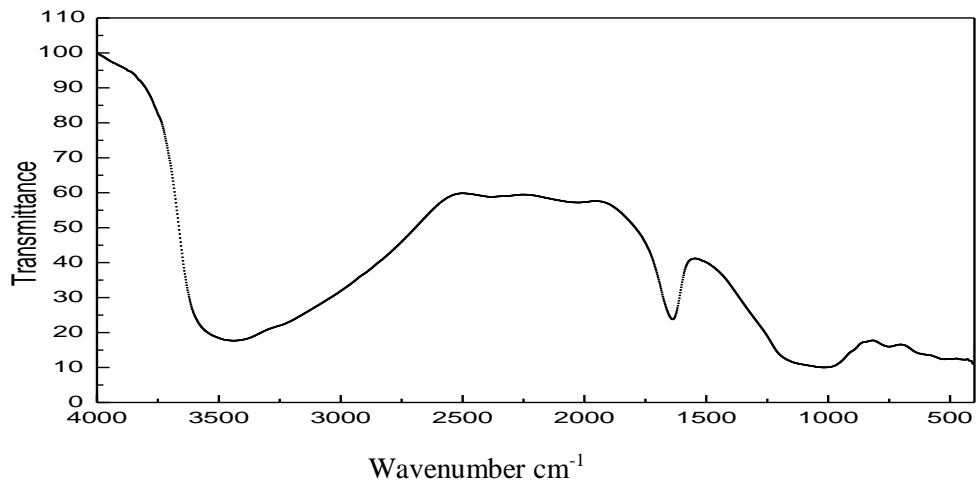


Fig.(4): IR spectrum of zirconium phosphate (ZP) composite.

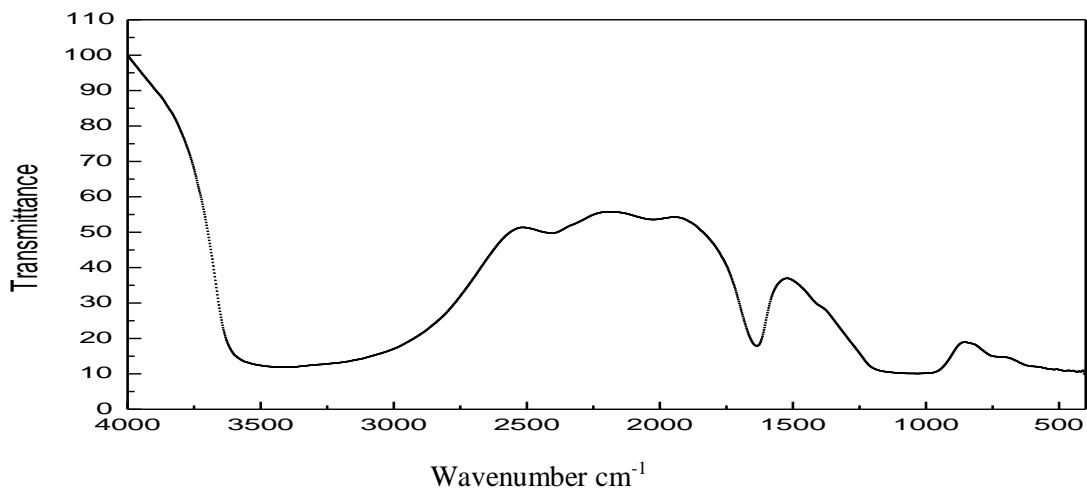


Fig.(5): IR spectrum of zirconium molybdate (ZM) composite.

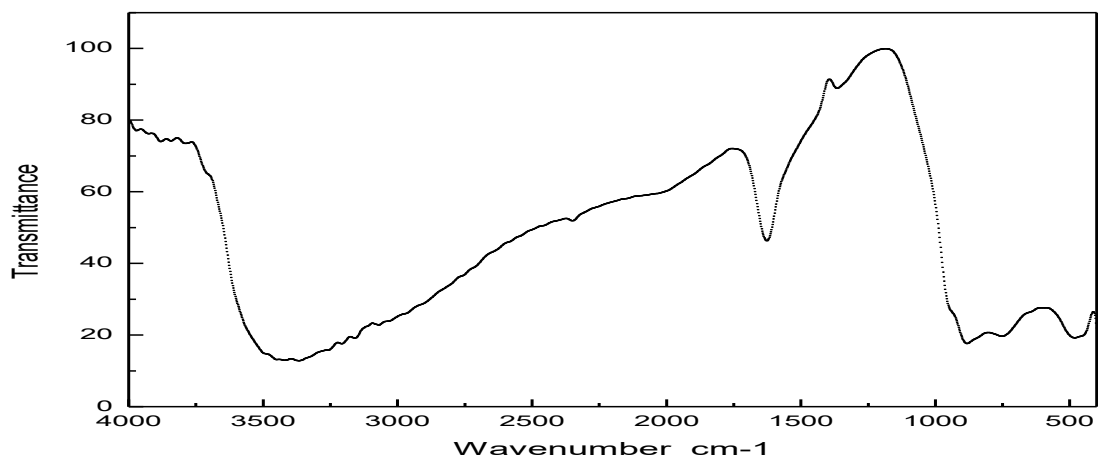


Fig.(6): IR spectrum of zirconium molybdo pyrophosphate (ZMPP) composite.

TGA and DTA of ZP, ZM and ZMPP composites are represented in Figs. (7-9) respectively. In figure (7) two endothermic peaks are appeared for ZP. The first at 91.860C due to dehydration of free water [7] and the second peak at 587°C due to start of condensation due to removal of lattice water from the material [1]. Figure (8) indicate 3 endothermic peaks at 121, 376.6 and 585.6°C for ZM. The first peak at 121°C may be due to removal of external water molecules and second peak at 376.6°C may be due to dehydration of interstitial water [7] and the last peak at 585.6°C due to the crystallization of ZrO₂ and MoO₃ to form ZrOMoO₄. Figure (9) indicate two endothermic peaks at 150°C and 596°C for ZMPP. The first peak at 150°C due to removal of external water molecules and the other peak at 596°C due to formation of pyrophosphate phase [7].An exothermic peak at 629°C were appeared due to the crystallization of ZMPP. From TG curves in figures (7-9),

the water content was calculated from the calcination of the composites at 850 °C. The data indicated that the weight loss of ZP, ZM and ZMPP were equal 20.4% ,10.52% ,11.3%, respectively. These values were used in calculation of the number of the water molecules in the composite material using the equation6 [6, 15];

$$18n = \frac{X(M+18n)}{100} \quad (8)$$

Where X is the percent weight loss of ignition and M is the molecular weight of the composite. The elemental analysis of the composites for Zr, Mo, P elements was carried out by X-ray fluorescence technique. From all results obtained from IR, LOI, XRD and XRF, the tentative formula of zirconium phosphate, zirconium molybdate and zirconiummolybdo pyrophosphate were assigned to be (Zr_{1.15}PO_{4.8.3H₂O}), (Zr_{1.18}Mo_{6.7.2H₂O}) and (Zr_{1.7}MoPO_{7.2.3H₂O}), respectively.

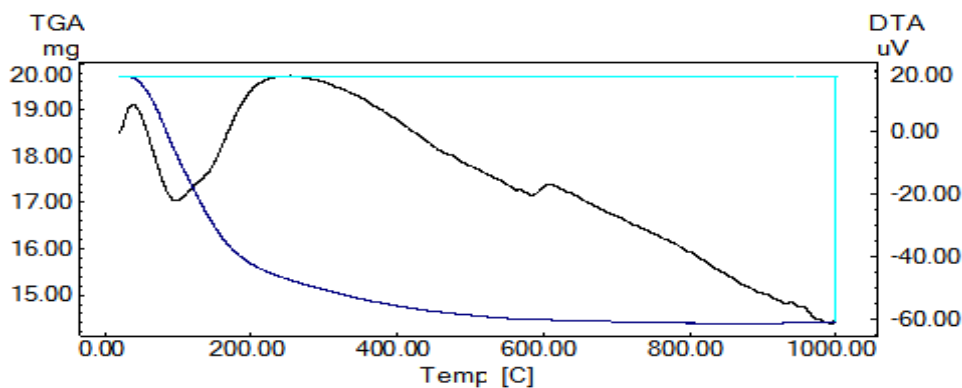
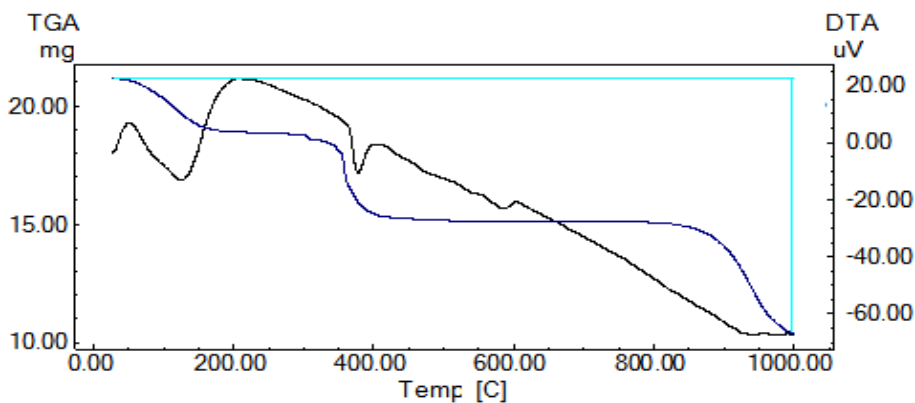
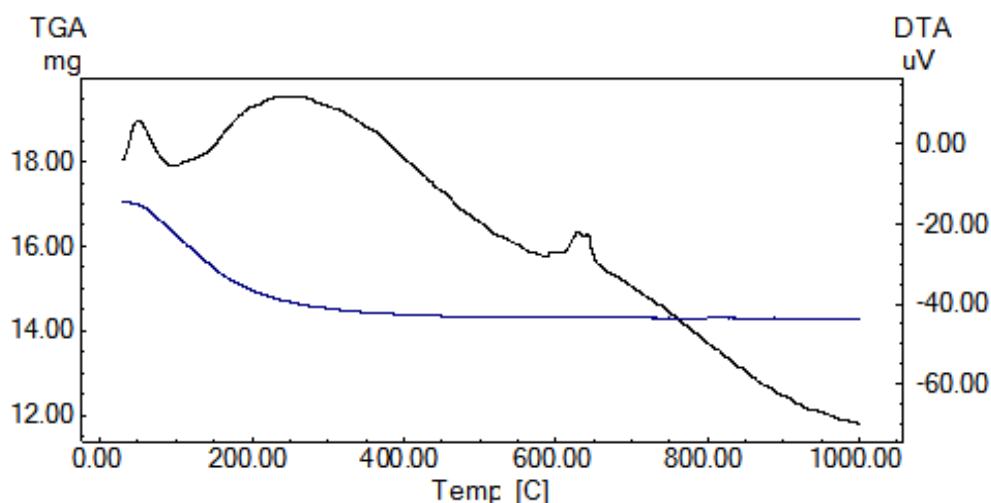


Fig.(7): DTA and TGA curves of zirconium phosphate composite.



Figs.(8):DTA and TGA curves of zirconium molybdate composite.



Figs.(9):DTA and TGA curves of zirconium molybdo pyrophosphate.

3.1- EFFECT OF HEATING TEMPERATURE ON THE APPARENT CAPACITY OF ZMPP COMPOSITE

Thermal treatment of zirconiummolybdo pyrophosphate was investigated by measuring the capacity of the composite at different heating temperatures that accompany the change in the structural behaviour. The capacity in mg/g was measured by batch technique using batch factor 100ml/g and metal ion concentration 30ppm. The data of capacity was represented in table (2) and showed that, generally, the original zirconium molybdo pyrophosphate composite dried at 50°C are selective for Pb²⁺ and Cd²⁺ ions. Water molecules play important roles as exchangeable active sites, on heating at

200°C, 600°C and 850°C the capacity of zirconium molybdo pyrophosphate decreased which may be attributed by in the early stage of the heating only water molecules present in the cavity of the exchanger will be lost (cavity water), and by increasing the heating temperature the water molecules present in the structure will be lost during condensation (condensation water) leading to shrinkage in the cavity and channels of the exchanger at higher temperatures. This shrinkage in the structure leading to some strike difficulties and decrease in the number of the exchangeable active sites of the exchanger [12].

Table (2): Effect of thermal treatment on capacity of zirconiummolybdopyrophosphate for Pb²⁺ and Cd²⁺ ions at 25±1°C.

Ion Exchanger	Heating Temperature, °C	Capacity mg/g	
		Pb ²⁺	Cd ²⁺
Zirconium molybdo pyro phosphate (Zr _{1.7} MoPO _{7.2} .3H ₂ O)	50	11.17	10.75
	200	10.45	9.71
	600	8.87	8.83
	850	8.05	8.42

4- REFERENCES

[1] S.A. Nabi , Mu. Naushad and Inamuddin, Synthesis and characterization of a new

inorganic ion-exchanger—Zr(IV) tungstomolybdate: Analytical applications for metal content determination in real sample and

- synthetic mixture, *Journal of Hazardous Materials* 142 (2007) 404–411.
- [2] M. Islama and R. Patel, Removal of lead (II) from aqueous environment by a fibrous ion exchanger: Polycinnamamide thorium (IV) phosphate, *Journal of Hazardous Materials* 172 (2009) 707–715.
- [3] A. Dabrowski, Z. Hubicki, P. Podkościelny and E. Robens, Selective removal of the heavy metal ions from waters and industrial wastewaters by ion-exchange method, *Chemosphere* 56(2004)91–106.
- [4] S.A. Shady and A.A. El-Sadek, Potential Use of Resorcinol-Formaldehyde and Zirconyl - Molybdo Pyrophosphate Ion – Exchange Materials for the Chromatographic Separation of Cesium, Cobalt and Europium Ions, *Arab Journal of Nuclear Science and Applications*, 46(4), (2013) 53-61
- [5] I.M El-Naggar M.M, Abou-Mesalam, M.M El-Shorbagy and S.A. Shady, Thermal and Chemical Stability of some synthesized Inorganic Ion Exchange Materials *Arab Journal of Nuclear Sciences and Applications*, 39(3), (2006).
- [6] M.M. Abou-Mesalam and M.M El-Shorbagy, Potassium Iodo-Zirconium Silicate Composite Material and Its Application for Retention of Cobalt, Cadmium and Copper Ion Pollutants, *Journal of Chemical Engineering and Chemistry Research* 1(1) (2014) 33-39.
- [7] M.M. Abou-Mesalam, Structural and Crystallographic Features of Chemically Synthesized Cerium-Titanium Cerium-Antimonates Inorganic ion Exchangers and Its Applications, *Advances in Chemical engineering and Science*, 1(2011)1-8.
- [8] M.M. Abou-Mesalam and I.M El-Naggar, Novel inorganic ion exchange materials based on silicates; synthesis, structure and analytical applications of magnesio-silicate and magnesium alumino-silicate sorbents, *Journal of Hazardous Materials* 149(2007) 686-692.
- [9] F. Gu, S.R. Wang, M. K. Lu, G.J. Zhou, D. Xu and D.R. Yuan, *Lungmuir*, 20(2004) 3258.
- [10] B.D. Cullity and S.R. Steck, *Elements of X-ray Diffraction*, 3rd Ed., Prentice-Hall, Englewood Cliffs, NJ (2001).
- [11] M.M. Abou-Mesalam, Evaluation of Crystalline size and Lattice Strain in Nano Particles of Transition Metals Hexacyanoferrate, *International Journal of advanced Chemical Technology*, 2(1) (2013) .
- [12] M.M. Abou-Mesalam, Hydrothermal Synthesis and Characterization of a Novel Zirconium Oxide and Its Application as an Ion Exchanger, *Advances in Chemical Engineering and Science*, 1(2011)20-25.
- [13] R. Thakkar and U. Chudasama, Synthesis and characterization of zirconium titanium phosphate and its application in separation of metal ions, *Journal of Hazardous Materials* 172 (2009) 129–137.
- [14] M.M. Abou-Mesalam, Sorption kinetics of copper, zinc, cadmium and nickel ions on synthesized silico-antimonate ion exchange, *Colloids and Surfaces A: Physicochem. Eng. Aspects* 225 (2003) 85-94.
- [15] W.A. Siddiqui and S.A. Khan, Synthesis, characterization and ion exchange properties of zirconium (IV) tungstoiodophosphate, a new cation exchanger, *Bull. Mater. Sci.*, 30(1) (2007) 43–49.